Published in final edited form as:
Exp Cell Res. 2009 August 1; 315(13): 2215–2230. doi:10.1016/j.yexcr.2009.03.020.

Transport of mannose-6-phosphate receptors from the trans Golgi network to endosomes requires Rab31

A.G. Rodriguez-Gabin[a], **X. Yin**[a], **Q. Si**[a], and **J.N. Larocca**[a,b]

[a] Department of Neurology, Albert Einstein College of Medicine, Yeshiva University, Bronx, NY, 10461

[b] Department of Neuroscience, Albert Einstein College of Medicine, Yeshiva University, Bronx, NY, 10461

Abstract

Rab31, a protein that we originally cloned from a rat oligodendrocyte cDNA library, localizes in the trans Golgi network (TGN) and endosomes. However, its function has not yet been established. Here we show the involvement of Rab31 in the transport of mannose 6-phosphate receptors (MPRs) from TGN to endosomes. We demonstrate the specific sorting of cation-dependent-MPR (CD-MPR), but not CD63 and vesicular stomatitis virus G (VSVG) protein, to Rab31-containing trans-Golgi network carriers. CD-MPR and Rab31 containing carriers originate from extending TGN tubules that also contain clathrin and GGA1 coats. Expression of constitutively active Rab31 reduced the content of CD-MPR in the TGN relative to that of endosomes, while expression of dominant negative Rab31 triggered reciprocal changes in CD-MPR distribution. Expression of dominant negative Rab31 also inhibited the formation of carriers containing CD-MPR in the TGN, without affecting the exit of VSVG from this compartment. Importantly, siRNA-mediated depletion of endogenous Rab31 caused collapse of the Golgi apparatus. Our observations demonstrate that Rab31 is required for transport of MPRs from TGN to endosomes and for the Golgi/TGN organization.

Keywords

membrane transport; carriers; Rab proteins; mannose-6-phosphate receptors; Golgi; trans Golgi network; endosomes; lysosomes

INTRODUCTION

Intracellular membrane trafficking is essential to maintain both the structural and functional organization of cells. An elaborate system of vesicle-tubular carriers is employed in communication among the compartments of the exocytic and endocytic pathways and the plasma membrane. This membrane transport governs the composition and size of the various cellular compartments and cell surface [1].

Membrane transport pathways are regulated by the concerted control of: 1) the formation and release of carriers, 2) the movement of carriers along elements of the cytoskeleton, and 3) the

Correspondence to: J.N. Larocca, Department of Neurology/Neuroscience, AECOM, 1300, Morris Park Ave., Bronx, NY, 10461, Tel: (718) 430-2831, FAX: (718) 430-2441, E-mail: larocca@aecom.yu.edu.

targeting and fusion of carriers [2,3]. Rab proteins are key components in these mechanisms of carrier formation, movement and carrier targeting [4]. The family of Rab proteins encompasses more than 70 members; each member regulates a specific vesicle trafficking pathway (Pfeffer, 2005). For example, Rab1 is involved in transport from the endoplasmic reticulum to the Golgi complex [5], Rab8 in transport from the trans Golgi network (TGN) to the plasma membrane [6], Rab3 in transport from synaptic vesicles to the plasma membrane [7], Rab5 in transport from the plasma membrane to early endosomes [8], Rab6 in transport from Golgi to endoplasmic reticulum [9], Rab7 in transport from late endosomes to lysosomes [10], and Rab 9 in transport from late endosomes to the TGN [11].

Despite numerous studies, the role of many Rab proteins remains unknown. A novel Rab protein we cloned from a rat oligodendrocyte cDNA library was designated rRab22b, because of its similarity to human Rab22b [12]. Its high degree of homology, ninety six percent, with human Rab22b indicates that rRab22b is the orthologue of human Rab22b. Subsequent publications by others identify Rab22b as Rab31 [13]. For consistency with the literature, we now refer to rRab22b as Rab31.

In a previous study, we found that Rab31 is localized in the TGN and endosomes. Rab31 partially co-localized with both early endosomal markers Rab5 and endocytosed transferrin (after incubation of cells for 5 min with Texas Red transferrin) [12]. The presence of Rab31 in TGN and early endosomes was recently corroborated by two other groups [14,15]. Indeed, Rab31 co-localized with syntaxin-6, a marker for TGN, and partially co-localized with EEA1, a marker for early endosomes.

We showed by time lapse video microscopy that Rab31 localized in tubulo vesicular carriers that bud from the TGN, travel along microtubules toward the cell periphery, and fuse with endocytic compartments [12]. These observations suggest the involvement of Rab31 in TGN to endosomes transport. However, the nature and biological significance of the Rab31 dependent membrane transport remain unknown.

Two distinctive membrane transport pathways transport newly synthesized proteins from the TGN to endocytic compartments. One pathway depends on both cation-dependent and cation-independent MPRs and transport lysosomal enzymes. Lysosomal hydrolases are transported to endosomes in a complex with MPRs [16]. In endosomes the complex dissociates, the hydrolases are delivered to the lysosomes, and the MPRs are then recycled to the TGN [17]. MPR-hydrolase complexes are transported from the TGN to endosomes in carriers coated with clathrin and the gamma ear containing, ADP ribosylation factor binding proteins (GGAs) [18,19]. GGAs contribute to the recruitment of the MPRs-hydrolase complexes to new carriers through interaction between the GGA1 VHS domain and the DXXLL signal in the cytosolic domain of MPRs [20].

The other pathway does not depend on MPRs and transports newly synthesized lysosome-associated membrane proteins (LAMPs), including LAMP-1, LAMP-2 and LAMP-3 (also known as CD63), [21–23]. CD63 is transported from TGN to lysosomes through a route involving passage through late endosomes. However, a fraction of newly synthesized CD63 may move from TGN to early endosomes before being targeted to lysosomes, and also via the plasma membrane [24]. Sorting of CD63 into carriers budding from the TGN appears to be mediated by the signal GYEVM that is present in its cytosolic domain.

In this study, we demonstrated the involvement of Rab31 in the transport of MPRs from the TGN to endosomes. Analysis by double fluorescence microscopy of HeLa cells co-expressing Rab31-EYFP and CD-MPR-ECFP show that CD-MPR-ECFP in the TGN is specifically sorted to carriers containing Rab31-EYFP. In contrast, newly synthesized CD63-EYFP and VSVG-EYFP are not sorted to Rab31 carriers. Our results also show that two coat proteins, clathrin

light chain b isoform and GGA1, co-localized with Rab31 in the TGN, carriers and peripheral tubulo vesicular structures. Expression of the mutant Rab31(S19N) inhibited the formation in the TGN of carriers containing CD-MPR. In contrast, expression of the mutant Rab31(Q64L) increased slightly the formation of carriers containing CD-MPR. Depletion of endogenous Rab31 causes collapse of the Golgi apparatus. This study indicates that Rab31 participates in both the transport of MPRs from TGN to endosomes and in the Golgi/TGN organization.

MATERIALS AND METHODS

Recombinant DNA Procedures

The cloning of Rab31 tagged with EYFP or ECFP was described previously [12]. Rab31(S19N) and Rab31 (Q64L)mutants were obtained by site–directed mutagenesis according to the method of Ho et al. [25].

The CD63-ECFP, CD63-EYFP, clathrin-ECFP, GGA1-ECFP and CD-MPR-ECFP expression plasmids were provided by Dr. Juan Bonifacino (Cell Biology and Metabolism Branch, National Institute of Child Health and Human Development, National Institutes of Health, Bethesda, MD 20892, USA). The VSVG-Venus expression plasmid was provided by Dr. Erik Snapp (Anatomy and Structural Biology Department, Albert Einstein College of Medicine, Yeshiva University).

Cell line cultures

HeLa cells (Epitheloid carcinoma, from human cervix, obtained from American Type Culture Collection) were maintained in MEM supplemented with 10% FCS, 1% essential amino acids, 2 mM glutamine, 100 U/ml penicillin and 100 μg/ml streptomycin at 37° C in a 5% CO_2 incubator.

For transfection experiments, HeLa cells were plated on 35-mm glass-bottom cultures dishes (MatTek Corporation, Ashland, MA) at a density of 0.4–1.6 X 10^5 cells per dish for 24 hours before transfection.

Transfection

HeLa cells were transfected using Lipofectamine Plus (GIBCO BRL, Gaithersburg, MD) according to the instruction of the manufacturer. Briefly, cultures were treated with 1.2 ml of growth medium containing 3 μg DNA, 12.5 μg of Lipofectamine and 10 μl of Plus reagent at 37° C for 3–6 hr. To select HeLa cells permanently transfected with pGolgi-ECFP, CD63-ECFP, MPR-ECFP and Rab31-ECFP, G418 (2 mg/ml) was added to the culture media, 48 hours after transfection.

Intranuclear injection of DNA

HeLa cells were pressure micro-injected intranuclearly with cDNAs prepared in KCl micro-injection buffer (10 mM Hepes, 140 mM potassium chloride at pH 7.4); 20 μg ml^{-1} for CD63-ECFP and 20 μg ml^{-1} for CD63-EYFP, using back-loaded glass capillaries and FenmtoJet micro pump and InjectMan micromanipulator (Eppendorf, Hamburg, Germany). After injection, cells were maintained at 37 °C in a humidified CO_2 environment for 60 min to allow for expression of injected cDNAs. Newly synthesized protein was accumulated in the TGN by incubating cells at 20 °C in bicarbonate-free MEM supplemented with 10% FCS, 1% essential amino acids, 2 mM glutamine, 100 U/ml penicillin and 100 μg/ml streptomycin, 20 mM Hepes and 100 μg ml^{-1} cycloheximide (Sigma, St Louis, MO). Cells were transferred to recording medium (bicarbonate and phenol-red -free MEM supplemented with 1% FBS, 20 mM Hepes, 1% essential amino acids, 2 mM glutamine, 100 U/ml penicillin and 100 μg/ml streptomycin and 100 μg ml^{-1} cycloheximide) and the transport and fusion of post-Golgi carriers was

monitored by time-lapse fluorescence microscopy after shifting to the permissive temperature for transport out of the Golgi (32° C).

Fluorescence microscopic analysis of living cells

Cells were imaged in recording medium at the temperatures indicated in the Figure legend using an Olympus IX70 inverted microscope with a 60X Olympus Planapo oil immersion objective NA 1.4 and equipped with a cooled CCD camera (Photometrics coolSNAP HQ, Roper Scientific) with a 2 × 2 binning. All imaging hardware was controlled by a workstation running I.P. Lab Spectrum imaging software (Scanalytics, Inc. Fairfax, VA). Cells expressing ECFP chimeras were excited using a 436 ± 20 nm filter (Chroma Technology) and imaged with a filter 480 ± 40 nm (Chroma Technology). The exciter filter 500 ± 20 nm, and the emitter filter 535 ± 30 nm (Chroma Technology) were used to visualize EYFP chimeras. Cells expressing both ECFP and EYFP chimeras were excited using a double band filter 436 ± 10 nm and 500 ± 10 nm (Chroma Technology), the emitted fluorescence was splinted using a bean splitter (Dual-View, Roper Scientific) and ECFP fluorescence imaged with a filter 465 ± 30 nm and EYFP fluorescence imaged with a filter 535 ± 30 nm. Out of focus haze was removed from the images by deconvolution (Scanalytics' IPLab image processing and analysis software).

Time lapse studies were carried out to analyze the dynamics of organelles; images were collected at the intervals indicated in the figure legend. At least 40 cells were analyzed per each experimental condition. Kymograph analysis was carried out using the ImageJ 1.36 software (Rasband, 1997–2007). Kymograph analysis of carrier formation and carrier movement was carried out by first defining the area of the cell that included the budding site in the TGN and the carrier trajectory. Second the fluorescence detected in the defined area was graphed as a function of the time and space. To evaluate quantitatively the level of colocalization, the Pearson's correlation coefficient (*r*) [26] was calculated, with one indicating complete positive correlation and zero indicating no correlation. Values were calculated using the image analysis software ImageJ 1.36b. To determine the distribution of CD-MPR intensities of CD-MPR-ECFP fluorescence in the TGN, and in peripheral compartments were measured. Fixed cells were optically sectioned along the z-axis at 0.5 μm intervals using a 60X Olympus Planapo oil immersion objective NA 1.4. After subtraction of background, image stacks were analyzed either without processing or after 3D deconvolution using I.P. Lab Spectrum imaging software (Scanalytics, Inc. Fairfax, VA) to remove out-of-focus fluorescence. Both methods gave similar results. The amount of MPR-ECFP present in the TGN and the peripheral compartments was expressed as percentage of the total fluorescence.

Velocity of VSVG-Venus exit from Golgi

HeLa cells were first transfected with plasmid encoding either wild type Rab31 or Rab31 (S19N) mutant or Rab31 (Q64L) mutant. Two days later, these cells were transfected with plasmid encoding VSVG-Venus, and maintained for 16 hours at 40° C. By incubating the cells at 20° C for 3 hours in the presence of cycloheximide, newly synthesized VSVG-Venus was trapped in the TGN. The cells were incubated at 32° C for 5, 10, 15, 20, 30, 40, 60, 90 and 120 min prior to fixation to permit transport of VSVG-Venus from TGN to the plasma membrane.

Intensities of fluorescence of the Golgi compartments (FG), and intensity of fluorescence of the entire cell (FC) were measured. Fixed cells were optically sectioned along the z-axis at 0.5 μm intervals using a 60X Olympus Planapo oil immersion objective NA 1.4. After subtraction of background, image stacks were analyzed either without processing or after 3D deconvolution using I.P. Lab Spectrum imaging software (Scanalytics, Inc. Fairfax, VA) to remove out-of-focus fluorescence. Both methods gave similar results. The amount of VSVG present in the Golgi was expressed as a ratio of FG to FC. The values were normalized using

1 as the value of the ratio at time zero. Non linear regression analysis (GraphPad Prism software, GraphPad Software, Inc.) showed that the data for exit velocity of VSVG-Venus from the Golgi could be fit to a first order kinetic.

RNA-mediated Interference (RNAi)

To be certain of the results, RNAi was performed using siRNAs (Ambion, Austin, Texas) that target three different regions of the human Rab31 sequence: 1) 5′-GGAUCACUUUGACCACCACAAC-3′, 2) 5′-GGAUGCUAAGGAAUACGCU-3′, and 3) 5′-GCAGGAUUCAUUUUAUACC-3′). Control experiments were performed with non targeting siRNA (Negative Control #1, Ambion). HeLa cells were transfected using siPORT™ NeoFX™ reagent (Ambion) according to the instruction of the supplier (Ambion), using a reverse transfection protocol. Briefly, cultures were trypsinaized and the cells collected by centrifugation. The pellet was resuspended in medium without FCS at a density of 2×10^5 cells/ml. Aliquots of 1.5 ml of cell suspension were added to a 35 mm Petri dish containing siRNA/siPORT NeoFX complexes (30 nM siRNA, final concentration). Cells were analyzed 48 hours after transfection. The expression of Rab31 and Rab9 were determined by immunoblot analysis using mouse monoclonal antibodies (ABCAM, Cambridge, MA, USA), while expression of Rab5 was determinate using rabbit polyclonal antibodies (Santa Cruz, Santa Cruz, California, USA). Expression of GAPDH was determined using mouse monoclonal antibody (Ambion). Immunoblot analysis was carried out according to Larocca and Almazan [27] using the SuperSignal West Dura reagent (Pierce, Rockford, IL, USA). The signals were quantified by densitometry.

RESULTS

Rab proteins localize to the sites at which they regulate the traffic events. Our previous studies showed that Rab31 is present in the TGN, in peripheral small tubular vesicles and endosomes, suggesting that Rab31 is involved in the traffic of membranes between TGN and endosomes [12]. However, to define its role it is necessary to establish which cargo proteins are transported through the Rab31 pathway.

Indeed, from the TGN, newly synthesized proteins are targeted to endocytic compartments through at least two membrane trafficking pathways. One pathway depends on MPRs and transports lysosomal enzymes. The other pathway does not depend on MPRs and transports lysosomal membranes proteins including CD63 [28].

Therefore, we carried several sets of experiments to analyze the dynamic of Rab31 carrier formation and to determine which cargo proteins are sorted to Rab31 carriers.

Rab31 carriers form from the TGN

The dynamics and formation characteristics of carriers containing Rab31 were studied by time lapse fluorescence microscopy of HeLa cells stably transfected with plasmid encoding Rab31-ECFP. The time lapse experiments were carried out at 32° C, a permissive temperature widely used in the study of post Golgi transport [29,30], which facilitated the visualization of the carrier formation from the TGN.

Rab31-ECFP localized in structures of the TGN (large vesicles and large tubular formations located close to the nucleus), and in small tubular vesicles located throughout the cytoplasm including the cell periphery (Fig. 1A). Analysis of time lapse images showed that large TGN tubular structures extend (up to 20 μm), from the cell center to the periphery. These tubular structures appeared to be flexible, to undulate while extending, and to bend while changing direction of movement. Kymographic analysis of data obtained in the time lapse experiments

showed that these tubular structures extend from the TGN towards the cell periphery at speeds that range from 0.30 to 1.27 μm/sec. (Fig. 1 and Video 1). Interestingly, we observed that tubular carriers break out from TGN extending tubules, but not from TGN tubules that are not extending.

Carriers containing Rab31-ECFP were of diverse size (0.2 μm to 5 μm long). Long tubular carriers formed when extending TGN tubules broke up in a region close to the TGN. Small tubular carriers formed when tips of extending TGN tubules broke up (Fig. 1B-D), and when these extending tubules broke up simultaneously into several parts. Alternatively, small tubular carriers formed from fragmented long tubular carriers (Video 1).

These tubular carriers moved toward the cell periphery along linear or curvilinear trajectories, at speeds ranging from 0.40 to 1.20 μm/sec. Movements were intermittent, with frequent changes in direction (Video 1). As they moved toward the cell periphery, the majority dropped out of the focal plane. However, some interacted and fused with small vesicles, which probably are part of the endosomal system (Video 1). To assess whether small tubular vesicles containing Rab31 were endosomal compartments, HeLa cells expressing Rab31-ECFP were allowed to internalize Texas Red transferrin for 15–20 min. As shown in Figure 2, a large number of Rab31-ECFP containing structures are in tight contact with transferrin-positive tubular vesicular structures (Figure 2). Furthermore, we observed that Rab31-ECFP and Texas Red transferrin co-localized in tubular compartments located in the cell periphery ($r = 0.815 \pm 0.047$) (Figure 2). These results strongly suggest that Rab31 carriers can interact and fuse with endocytic compartments containing internalized transferrin.

Rab31 carriers contain CD-MPR

As we observed with Rab31 carriers, Waguri et al. [31] showed that MPRs are transported in tubular carriers that detach from the TGN and fuse with endocytic compartments containing endocytosed transferrin. To assess if CD-MPR is sorted to Rab31 containing carriers budding from TGN, HeLa cells stably transfected with plasmid encoding CD-MPR-ECFP were transfected with plasmid encoding Rab31-EYFP. Cells expressing both proteins were examined by double fluorescence microscopy.

The results showed that both CD-MPR-ECFP and Rab31-EYFP co-localized in structures of the TGN ($r = 0.807 \pm 0.044$), and in small tubular compartments located throughout the cytoplasm ($r = 0.745 \pm 0.064$) (Fig. 3A).

We observed tubular carriers containing both Rab31-EYFP and CD-MPR-ECFP forming from extending large tubular TGN structures (Fig. 3B and C). These carriers had kinetic and plastic properties similar to those containing only Rab31-EYFP.

CD-MPR is specifically sorted to Rab31 carriers in the TGN

To assess if CD-MPR-ECFP is selectively sorted to carriers containing Rab31, we determined whether CD63, a protein transported to endosomes by an MPR-independent pathway, is sorted into Rab31 carriers.

HeLa cells stably transfected with plasmid encoding Rab31-ECFP were transiently transfected with plasmid encoding CD63-EYFP by intranuclear injection. Newly synthesized CD63-EYFP was trapped in the Golgi/TGN by incubating the cells for 3 hours at 20° C in the presence of cycloheximide.

CD63-EYFP and Rab31 partially colocalized in Golgi/TGN compartments ($r = 0.637 \pm 0.058$) (Fig. 4A-C). Some Golgi/TGN compartments seem to contain both proteins, while other compartments contained only one or the other (Fig. 4A-C). In contrast, carriers that bud from

the TGN contain only one fluorescent protein. Fig. 4E-G shows the formation of carriers containing only CD63-EYFP, or only Rab31-ECFP. Supplementary Fig. 2, shows the formation of a carrier containing CD63-EYFP.

Time lapse maximum pixel projection images clearly show that there is no colocalization of CD63-EYFP and Rab31-ECFP in carrier vesicles or endocytic compartments ($r = 0.174 \pm 0.058$) (Fig. 4D). In summary, we showed that newly synthesized CD63-EYFP is not recruited to tubular carriers containing Rab31-ECFP.

To further assess the specificity of sorting, we also studied the recruitment of VSVG to Rab31 carriers. HeLa cells expressing Rab31-ECFP were transfected with plasmid encoding VSVG-Venus (VSVG protein from the ts045 mutant strain of vesicular stomatitis virus was used), and were incubated at 40° C for 10–12 hrs. to accumulate VSVG-Venus in the ER [32]. Transfected cells were then incubated at 20° C for 3 hrs, with cycloheximide (100 μg/ml) to trap VSVG-Venus in the TGN. The cells were then transferred to recording media at 32 ° C to induce transport of VSVG from Golgi to PM. Time lapse photographs visualized the formation of carriers containing Rab31-ECFP and of carriers containing VSVG-Venus.

Our results showed that VSVG is not sorted in the TGN to carriers containing Rab31. VSVG-Venus and Rab31-ECFP co-localized in Golgi/TGN compartments ($r = 0.835 \pm 0.074$) (Fig. 5A-C). In contrast, carriers budding from the TGN contained only a single fluorescent protein. Fig. 5 shows the formation of carriers containing either VSVG-Venus (Fig. 5E-G), or Rab31-ECFP (Fig. 5H-J) but not both. These observations were confirmed by time lapse images (maximum pixel projection) that clearly showed no colocalization of VSVG-Venus and Rab31-ECFP in either carrier vesicles or endocytic compartments ($r = 0.213 \pm 0.076$) (Fig. 5D).

Using HeLa cells expressing both Rab31-EYFP and pGolgi-ECFP (a chimera constructed with ECFP and an 81 amino acid fragment of the N terminal region of human 1,4 beta galactosyl transferase, a protein that localized in Golgi/TGN)[33] we showed in time lapse studies that pGolgi is not recruited to Rab31 carriers (Supplementary Figure 1).

In summary, these results indicate that CD-MPR is sorted to Rab31 containing carriers in the TGN. Our data further indicate that three other proteins (pGolgi, newly synthesized CD63 and newly synthesized VSVG) are excluded from carriers containing Rab31. These observations demonstrated that CD-MPR is sorted selectively to Rab31 carriers.

Clathrin and GGA1 are present in Rab31 containing carriers

The previous results prompted us to investigate whether Rab31 co-localized with molecules such as clathrin and GGA1, which are involved in the gathering and sorting of MPRs to carriers in the TGN [34].

For this purpose, cells permanently transfected with plasmid encoding clathrin-ECFP (light chain) were transfected with Rab31-EYFP. Cells were examined by double fluorescence microscopy. Clathrin-ECFP and Rab31-EYFP were found to colocalize both in the TGN ($r = 0.967 \pm 0.043$), and in small vesicles located throughout the cytoplasm including the cell periphery ($r = 0.848 \pm 0.037$) (Fig. 6A–C). That the small Rab31/clathrin-containing vesicles are carriers is indicated by the budding of some of these vesicles from the TGN (Fig. 6D-F, Video 6).

Analysis of HeLa cells coexpressing GGA1-ECFP and Rab31-EYFP showed that both Rab31 and GGA1 are present in carriers budding from the TGN (Fig. 7 and Video 7). These observations further support the involvement of Rab31 in the transport of CD-MPR from TGN to endosomes.

Expression of Rab31 mutants (S19N) and (Q64L) changes both the distribution of CD-MPR (between the TGN and peripheral compartments) and the frequency of formation of CD-MPR carriers from the TGN

The capacity of Rab proteins to regulate membrane vesicle transport depends on their ability to alternate between two conformational states: GDP-bound (inactive) and GTP-bound (active), and their capacity to bind reversibly to specific compartments, inactive state for donor compartment, and active state for acceptor compartment. The normal nucleotide cycle of Rab proteins can be altered by expression of inactivated or activated mutant variants. It has been shown that inactivated mutant acts as dominant negative. In contrast, activated mutant is thought to support the activity of the endogenous Rab proteins.

Mutagenesis of specific amino acid residues within the three conserved motifs, phosphate/Mg (PM) loop 1 (Ser/Thr to Asn), G2 (Asn to Ile), and PM3 (Gln to Leu) perturb the cycle of guanine nucleotide binding or GTP hydrolysis [35–38]. Indeed, this approach has been extensively used to generate both inactivated and active mutants. Substitution of N for S in the last residue of PM (S25N mutant) of Rab1 produces a protein that is restricted to the GDP-bound state, a condition that inhibits both vesicle budding from the endoplasmic reticulum and transport of VSVG [39]. Mutations equivalent to the Q61L mutation in Ras decrease the GTPase activity of Rab mutant proteins. The defect in GTP hydrolysis in mutant Rab proteins may lead to stimulation of membrane transport [10].

Therefore, we used dominant negative and active mutants to define the role of Rab31 in the transport of CD-MPR from the TGN to endosomes. This role was assessed by examining their effect on the distribution of CD-MPR-ECFP between TGN and small tubular vesicles present throughout the cytoplasm, and their effect on formation of CD-MPR-ECFP containing carriers from the TGN. These experiments are based on the fact that CD-MPR cycles between TGN and endosomal compartments. Thus, changes in the TGN to endosomes transport should affect the distribution of CD-MPR between TGN and endosomes.

Dominant negative [Rab31(S19N)] and constitutively activated [Rab31(Q64L)] mutants were expressed as EYFP fusion proteins in HeLa cells expressing CD-MPR-ECFP. Two days after transfection the distribution of CD-MPR-ECFP between TGN and small tubular vesicles was analyzed by fluorescent microscopy.

In cells expressing wild type Rab31, 69.00 ± 2.00 % of the fluorescence of the CD-MPR-ECFP was localized in the TGN and 31.00 ± 2.00 % in small tubular vesicles.

Rab31(Q64L) expression shifted the distribution of CD-MPR, so that 41.00 ± 4.00 ($p < 0.001$) of the MPR-ECFP localized in the TGN and 59.00 ± 4.00 % ($p < 0.001$) of CD-MPR-ECFP in the small tubular vesicles. The TGN compartments containing CD-MPR were reduced in size, whereas small tubular vesicles appeared to be localized mainly near the cell periphery (Fig. 8G-I).

Expression of Rab31(Q64L)-EYFP did not affect the kinetic and plastic properties of the TGN compartments containing CD-MPR-ECFP (Video 8 I). The number of carriers formed in these cells (6.43 ± 1.02) was only slightly higher than in cells expressing wild type Rab31 (Table 1).

In contrast, the expression of Rab31(S19N) increased the amount of CD-MPR-ECFP in the TGN (84.00 ± 2.00 % vs 69.00 ± 2.00 %, $p < 0.001$) and reduced the CD-MPR-ECFP in peripheral compartments (16.00 ± 2.00 % vs 31.00 ± 2.00 %, $p < 0.001$). The amount of Rab31-EYFP in the cytoplasm seemed to be higher than the amount of wild type Rab31-EYFP (not shown). Expression of this mutant increased the size of the TGN compartment containing CD-MPR (Fig. 8D and F). In some cells the TGN is composed of long tubular structures (up to 20

μm long) (Fig. 8D-F). Expression of this mutant also caused changes in the appearance of the CD-MPR-ECFP containing compartments of the TGN. The large tubular compartments of TGN are largely immobile, and these structures do not extend or bend (Video 8 F) in contrast to cells transfected with wild type Rab31 (Video 8 C). Expression of this mutant dramatically reduced the formation of carriers containing CD-MPR from the TGN. In cells expressing Rab31 (S19N) less than one carrier (0.52 ± 0.09) is formed per 2 min period whereas 5.55 ± 0.09 carriers are formed in this period in wild type (Table 1). These carriers had kinetic and plastic properties similar to those of wild type Rab31-EYFP containing carriers.

Experiments were carried out to determine if the expression of Rab31 mutants specifically affect the formation of CD-MPR carriers. For this purpose the effect of Rab31 mutants on the exit of VSVG-Venus from the TGN was assessed. HeLa cells were transfected with plasmids encoding either wild type Rab31 or Rab31 (S19N), or Rab31(Q64L). Two days later, cells were transfected with plasmid encoding VSVG-Venus, and held for 16 hours at 40° C, prior to treatment with cycloheximide (3 hrs, 20° C). The cells were then incubated at 32° C for several time periods to permit the transport of VSVG-Venus from TGN to plasma membrane.

To assess the rate of exit of VSVG-Venus from the Golgi, the amount of fluorescence present in the Golgi (FG) and the entire cell (FC) were determined by fluorescense microscopy. The amount of VSVG-Venus present in the Golgi was expressed as the ration FG/FC, and the values normalized to 1 corresponding to time zero.

Non linear regression analysis yielded first order kinetics for the exit velocity of VSVG-Venus from the Golgi (Fig. 9). The results showed that the expression of Rab31 (S19N) or Rab31 (Q64L) mutants had no effect on the exit of VSVG-Venus from the Golgi (Fig. 9).

These observations confirm the involvement of Rab31 in the transport of CD-MPR from TGN to endosomes and suggest Rab31 is involved in the formation of carrier vesicles in the TGN.

Depletion of endogenous Rab31 causes collapse of the Golgi apparatus

The role of Rab31 was further analyzed by using siRNA to deplete endogenous Rab31. Treatment of cells with siRNA that target the sequence present in exon 2 (5′-GGAUCACUUUGACCACCACAAC-3′), reduced the expression of Rab31 by 95.00 ± 2.00 % (Fig. 10C, F and I). Since the expression of GAPDH did not change (Fig. 10C, F and I), the effect is specific.

Surprisingly, fluorescence microscopy showed that the depletion of Rab31 caused collapse of the Golgi/TGN structure in cells expressing pGolgi-ECFP (a chimeric protein constructed with ECFP and an 81 amino acid fragment of terminal region of human 1,4 beta galactosyl transferase, that localizes mainly in the trans-Golgi) [33]. The Golgi/TGN breaks up into vesicles (Fig. 10B). In contrast, the cells treated with non-targeting siRNA showed no alteration of Golgi/TGN structure, i.e. pGolgi localized in perinuclear tubular structures (Fig. 10A). These results suggest that the observed fragmentation of the Golgi is caused by depletion of Rab31 and is not a non specific effect of siRNA treatment. “Off-target effect” is not in consideration because treatment of the cells with two other siRNAs that target different segments of the Rab31 sequence [5′-GGAUGCUAAGGAAUACGCU-3′ (present in exon 6) and 5′-GCAGGAUUCAUUUUAUACC-3′ (present in exons 4 and 5)] also selectively depleted Rab31 and caused Golgi fragmentation (results not shown). Moreover, siRNA treatment did not inhibit expression of other Rab proteins including Rab5 and Rab9 (Supplementary Fig. 3).

Collapse of the TGN was also observed in cells expressing CD-MPR-ECFP when Rab31 was depleted. As shown in Fig. 10E, after 48 of the siRNA treatment, fragments of the TGN

containing CD-MPR are dispersed throughout the cell cytoplasm in these cells. Indeed, the breaking of the TGN structure can be observed at 36 hours after treatment. At this time the fragmentation of TGN structures seems to begin (Supplementary Fig. 4).

One cause of Golgi/TGN collapse would be inhibition of the activation of ARF1, a small GTPase involved in the recruitment to the TGN of clathrin adaptor proteins (AP-1, AP-3, AP-4 and GGAs)[40]. Therefore, we determined if depletion of Rab31 affects the recruitment of GGA1 to the Golgi. In cells expressing GGA1-ECFP whose Rab31 was depleted, we examined the binding of GGA1-ECFP to the Golgi. As shown in Fig. 10H, GGA1-ECFP is present in Golgi fragments dispersed throughout the cytoplasm. However, the amount of GGA1-ECFP bound to compartments did not change (80.00 ± 10.00 % in cells depleted of Rab31 versus 78.50 ± 7.00 % in control cells). Therefore, Golgi/TGN collapse is probably not due to inhibition of ARF1 activation and its recruitment of adaptor proteins.

In summary, these observations show that Rab31 is essential for maintaining the structure of the Golgi/TGN. They also show that Rab31 is not involved in the recruitment of GGA1 to TGN.

DISCUSSION

In this paper we show that Rab31 is part of the molecular mechanisms that regulate the transport of MPRs from the TGN to endosomes. Our results suggest that Rab31 participates in the formation of carrier vesicles in the TGN. Our observations also show that Rab31 is also involved in maintaining the structure of the Golgi/TGN.

The MPR transport pathway is used to transport newly synthesized endosomal and lysosomal proteins from the TGN to endosomes. This pathway is also traveled by certain proteins, such as sortilin, beta secretase and transferrin receptor [41,42], that are transported from the TGN to endosomes before reaching the cell surface. Indeed, this transport connects biosynthetic pathways to endocytic pathways, and plays an essential role in the biology of the cells, since it is involved in the biogenesis of endosomes, lysosomes and plasma membrane.

The involvement of Rab31 in the MPR pathway and in the Golgi/TGN structure was analyzed using four different criteria: a) Analysis of the sorting of cargo proteins to Rab31 carriers in the TGN; b) Determination of the presence in Rab31 carriers of proteins involved in the recruitment of cargo proteins; c) Effect of the expression of Rab31 mutants on both the formation of carriers and the distribution of cargo proteins between TGN compartments and peripheral compartments; d) Analysis of the effect of depletion of endogenous Rab31 by siRNA treatment.

CD-MPR is sorted to Rab31 carriers in the TGN, but not CD63

Our results showed that tubular carriers containing Rab31-ECFP form from TGN tubules. These carriers were of diverse size (0.2 μm to 5 μm long), and they break up from extending TGN tubules at velocities consistent with microtubule based motility, suggesting that both the formation and movement of carriers containing Rab31 involve microtubule based motors. Indeed, it was proposed that microtubule based motors mediate the generation of Golgi-derived carriers [43]. We visualized the formation of post TGN carriers by time lapse fluorescent microscopy of living cells incubated at 32° C. However, it should be noted that similar observations were obtained in studies carried out at 37° C [31].

Rab31 carriers make contacts, and possibly fuse with peripheral tubulo vesicular structures that contain endocytosed transferrin. These observations suggest that Rab31 carriers are involved in the delivered of newly synthesized proteins from the TGN to endosomes. This

hypothesis is supported by double fluorescence microscopy studies that showed that Rab31-EYFP carriers breaking up from the TGN contain CD-MPR-ECFP.

In contrasts, our results showed that newly synthesized CD63 is not sorted to Rab31 carriers in the TGN. Although Rab31-ECFP and CD63-EYFP partially co-localize in the TGN, only carriers that contain either Rab31-ECFP or CD63-EYFP break out from extending TGN tubules. Therefore, sorting of these two proteins occurs in the TGN before the carriers break out. Two alternative possibilities can be envisioned: 1) Rab31 and newly synthesized CD63 are sorted laterally into different domains of the same TGN cisternae, or 2) Rab31 and CD63 are sorted to adjacent TGN cisternae. The second possibility is supported by the fact that the TGN encompasses three cisternae, of which only the trans most is coated with clathrin [44].

Our conclusion that MPRs are specifically transported by Rab31 carriers is further supported by results showing that both a Golgi resident protein (pGolgi) and a protein targeted to the PM (VSVG) are not sorted into Rab31 carriers.

Rab31 carriers contain molecules involved with the gathering and sorting of MPRs to carriers

The involvement of Rab31 in the transport of MPRs is further supported by our results showing that Rab31 and clathrin co-localize in compartments of the TGN as well as in carriers. Complexes of MPRs-hydrolase gather within clathrin coated domains of the TGN before being packed into clathrin coated carriers for delivery to endosomal compartments [45].

Furthermore, our data show that Rab31 and GGA1 co-localize in the TGN and in carriers that bud from the TGN. These observations are consistent with the role GGA1 plays in transport of MPRs from TGN to endosomes. GGA1 is involved both in the gathering of MPRs and in the formation of clathrin coated carriers [40,46]. Indeed, GGA1 is clearly detected on carriers originating from the TGN and containing CD-MPR.

Expression of Rab31 mutants affects both carrier formation and distribution of CD-MPR present in the TGN and peripheral compartments

We find that the majority of the membrane associated Rab31(S19N) mutant is present in the TGN, suggesting that this GDP-locked Rab31 mutant interacts preferentially with effector proteins present in the TGN.

There is more than one model that explains the effect of the dominant negative mutant. It is possible that Rab31(S19N) might sequester GEF (guanine nucleotide exchange factor), so endogenous Rab31 protein can no longer be activated. Alternatively, the effect of dominant negative mutant can be explained by a model in which both conformational states of Rab31, GDP-bound and GTP-bound, interact with effectors, but only the GTP-bound form of Rab31 can activate the effectors. Although no yet proved, this hypothesis can be envisioned given that both conformational forms of Rab31 interact with OCRL-1, and that Rab31 and OCRL-1 co-localize in the TGN and in carriers budding from the TGN [47]. OCRL-1 is a member of group II inositol polyphosphate 5-phosphatases. Synaptojanin, another member of this group, is involved in synaptic vesicle budding by hydrolysis of a phosphate from $PI(4,5)P_2$ to produce PI(4)P [48].

Indeed, expression of Rab31 (S19N) dramatically reduced the formation of carriers containing CD-MPR from the TGN. Concomitantly, and probably as a consequence of the inhibition of the exit of CD-MPR from the TGN, the amount of CD-MPR increased in the TGN and decreased in endosomes. However, the formed carriers had kinetic characteristics similar to those of carriers containing wild type Rab31-EYFP. This observation is consistent with the dependence on endogenous Rab31 for formation of the carriers in cells expressing Rab31 (S19N). Additionally, expression of this mutant causes significant changes in the morphology

and dynamic of the TGN. The large tubular compartments of TGN are largely immobil; these structures do not extend or bend in contrast to cells transfected with wild type Rab31.

The Rab31(S19N) did not alter the exit of VSVG from the Golgi, indicating that this mutant affects specifically the CD-MPR transport. In apparent disagreement with our results, it was recently reported that expression of Rab31(S19N) mutant alters the exit of VSVG from the Golgi/TGN [49]. The reason for this apparent contradiction is not clear, but it may be due to differences in the level of mutant expressed.

Our observations are consistent with evidence showing that cytoplasmic Rab proteins are recruited to donor compartments in their inactive form [50], and that their activation is necessary for carrier formation [39]. The role of Rab proteins depends on recruitment of molecules such as cargo proteins, proteins involved in the targeting/fusion, and motor proteins [51–53]. In the TGN the recruitment of motor proteins by Rab31 is suggested by the observation that expression of Rab31(S19N) results in immobilization of TGN tubules containing CD-MPR.

In contrast to Rab31(S19N), Rab31(Q64L) reduced the amount of CD-MPR in the TGN whereas the amount of CD-MPR in peripheral compartments was increased. Additionally, Rab31(Q64L) causes accumulation in the cell periphery of small vesicles containing both Rab31(Q64L) and CD-MPR. A slight increase in the formation of carriers containing CD-MPR was also observed.

These observations indicated that Rab31(Q64L) has a dominant-active effect on the function of Rab31. The accumulation of Rab31(Q64L) in peripheral compartments is in agreement with evidence that active Rab proteins remain bound to the acceptor compartment. Recycling to the cytoplasm required hydrolysis of GTP [51]. Regarding the possible involvement of Rab31 in the recruitment of motor proteins, it is of interest to note that similarly to the expression of Rab31(Q64L), expression of the KIA13A (a motor involved in the movement of MPRs carriers) produced accumulation of compartments containing MPRs in the cell periphery [54].

Specifically, our observations demonstrate the involvement of Rab31 in the transport of MPRs from the TGN to endosomes. Additionally, we find that Rab31 is involved in the formation of the carriers. However, Rab31 may also participate in movement and targeting of MPRs carriers to endosomes.

Rab31 is involved in maintaining Golgi/TGN structure

As to the role of Rab31 in maintaining the Golgi/TGN structure, its depletion results in collapse. Golgi/TGN tubular structures after fragmentation disperse throughout the cytoplasm. The break up of the Golgi/TGN structures was observed in three cell lines expressing different fluorescent fusion proteins including pGolgi (a fusion protein of the 1,4 beta galactosyl transferase and ECFP), CD-MPR-ECFP and GGA1-ECFP. At early stage, the TGN compartments containing CD-MPR-ECFP or GGA1-ECFP begin to break up in rather large vesicles. However at later stages the remaining TGN fragments are of smaller size and they are dispersed in the cytoplasm. In cells expressing pGolgi fragmentation also occurs but the remaining Golgi compartments seem to disperse less than the compartments containing CD-MPR-ECFP or GGA1-ECFP. It is possible that this difference is due to the fact that pGolgi is localized in a different domain than CD-MPR and GGA1. Indeed, depletion of the membrane–tethering protein p115 results in disruption of the Golgi/TGN structure. Similarly to our observations, proteins that originally localized in the *cis* and *medial* Golgi including GM130, GPP130 and giantin localized in fragmented Golgi compartments that remain in the perinuclear region. In contrast, the TGN is split into structures disperse throughout the cell, as visualized by the detection of TGN46 [55].

The phenotype caused by depletion of endogenous Rab31 is different from that caused by expression of Rab31 mutants [Rab31(S19N) and Rab31(Q64L)]. It is not yet possible to explain how the different phenotypes are originated. However, our results suggest that both conformational states of Rab31 (GTP-bound and GDP-bound) are involved in maintaining the structure of the Golgi/TGN, and that Rab31's role depends on its interaction with more than one effector. While active Rab31 (GTP-bound) might be involved in the extension of the TGN tubules and formation of the carriers, the non active Rab31 (GDP-bound) might participate in the recruitment of cytosolic proteins involved in the Golgi/TGN structure. Certainly Rab31 (S19N) localizes mainly in the Golgi/TGN. Alternatively, it is also possible that the phenotype observed in cells over-expressing Rab31 dominant negative is determined in part by the presence of endogenous Rab31. Additionally, our results showed that Golgi/TGN collapse is not the result of disruption of recruitment of coat adaptor proteins by inhibition of ARF1 activation.

Our observations are in agreement with the role of Rab proteins as organizers of membrane domains [51]. It has been proposed that Rab proteins and their cognate effectors are spatially segregated in defined membrane domains. These effector interactions play an important role in domain organization. In the proposed model the organization of the Golgi/TGN domains require Rab31 and the other Rab proteins present (Rab1, 2, 6, 8, 10, 12, 13, 30, 33 and 36) [56,57]. Evidence shows that Rab1 and Rab6a are involved in Golgi stability.

In summary, this study indicates that Rab31 participates in both Golgi/TGN organization and in the transport of MPRs from TGN to endosomes. These observations contribute to the understanding of the biogenesis of the Golgi/TGN, endocytic and lysosomal compartments.

Supplementary Material

Refer to Web version on PubMed Central for supplementary material.

Acknowledgments

We thank Dr. Maurice Rapport and Dr. Teresa DiLorenzo for editing and commenting on the article. We thank Mr. Michael Cammer, Director of light Microcopy and Image Analysis, for his valuable help in processing of the cell images. This work was supported by NIH grant RO1 NS 47500-01 to J.N.L. Y. X. and S. Q. were supported by NIH training grant NS 07098.

References

1. Rohn WM, Rouille Y, Waguri S, Hoflack B. Bi-directional trafficking between the trans-Golgi network and the endosomal/lysosomal system. J Cell Sci 2000;113 (Pt 12):2093–2101. [PubMed: 10825282]
2. Rothman JE. Mechanisms of intracellular protein transport. Nature 1994;372:55–63. [PubMed: 7969419]
3. Bonifacino JS, Glick BS. The mechanisms of vesicle budding and fusion. Cell 2004;116:153–166. [PubMed: 14744428]
4. Armstrong J. How do Rab proteins function in membrane traffic? Int J Biochem Cell Biol 2000;32:303–307. [PubMed: 10716627]
5. Plutner H, Cox AD, Pind S, Khosravi-Far R, Bourne JR, Schwaninger R, Der CJ, Balch WE. Rab1b regulates vesicular transport between the endoplasmic reticulum and successive Golgi compartments. J Cell Biol 1991;115:31–43. [PubMed: 1918138]
6. Huber LA, Pimplikar S, Parton RG, Virta H, Zerial M, Simons K. Rab8, a small GTPase involved in vesicular traffic between the TGN and the basolateral plasma membrane. J Cell Biol 1993;123:35–45. [PubMed: 8408203]
7. Sudhof TC. The synaptic vesicle cycle. Annu Rev Neurosci 2004;27:509–547. [PubMed: 15217342]

8. Bucci C, Parton RG, Mather IH, Stunnenberg H, Simons K, Hoflack B, Zerial M. The small GTPase rab5 functions as a regulatory factor in the early endocytic pathway. Cell 1992;70:715–728. [PubMed: 1516130]
9. White J, Johannes L, Mallard F, Girod A, Grill S, Reinsch S, Keller P, Tzschaschel B, Echard A, Goud B, Stelzer EH. Rab6 coordinates a novel Golgi to ER retrograde transport pathway in live cells. J Cell Biol 1999;147:743–760. [PubMed: 10562278]
10. Bucci C, Thomsen P, Nicoziani P, McCarthy J, van Deurs B. Rab7: a key to lysosome biogenesis. Mol Biol Cell 2000;11:467–480. [PubMed: 10679007]
11. Lombardi D, Soldati T, Riederer MA, Goda Y, Zerial M, Pfeffer SR. Rab9 functions in transport between late endosomes and the trans Golgi network. EMBO J 1993;12:677–682. [PubMed: 8440258]
12. Rodriguez-Gabin AG, Cammer M, Almazan G, Charron M, Larocca JN. Role of rRAB22b, an oligodendrocyte protein, in regulation of transport of vesicles from trans Golgi to endocytic compartments. J Neurosci Res 2001;66:1149–1160. [PubMed: 11746448]
13. Bao X, Faris AE, Jang EK, Haslam RJ. Molecular cloning, bacterial expression and properties of Rab31 and Rab32. Eur J Biochem 2002;269:259–271. [PubMed: 11784320]
14. Lodhi IJ, Chiang SH, Chang L, Vollenweider D, Watson RT, Inoue M, Pessin JE, Saltiel AR. Gapex-5, a Rab31 guanine nucleotide exchange factor that regulates Glut4 trafficking in adipocytes. Cell Metab 2007;5:59–72. [PubMed: 17189207]
15. Ng EL, Wang Y, Tang BL. Rab22B's role in trans-Golgi network membrane dynamics. Biochem Biophys Res Commun 2007;361:751–757. [PubMed: 17678623]
16. Kornfeld S. Trafficking of lysosomal enzymes. FASEB J 1987;1:462–468. [PubMed: 3315809]
17. Le Borgne R, Hoflack B. Mechanisms of protein sorting and coat assembly: insights from the clathrin-coated vesicle pathway. Curr Opin Cell Biol 1998;10:499–503. [PubMed: 9719871]
18. Doray B, Ghosh P, Griffith J, Geuze HJ, Kornfeld S. Cooperation of GGAs and AP-1 in packaging MPRs at the trans-Golgi network. Science 2002;297:1700–1703. [PubMed: 12215646]
19. Puertollano R, van der Wel NN, Greene LE, Eisenberg E, Peters PJ, Bonifacino JS. Morphology and dynamics of clathrin/GGA1-coated carriers budding from the trans-Golgi network. Mol Biol Cell 2003;14:1545–1557. [PubMed: 12686608]
20. Bonifacino JS. The GGA proteins: adaptors on the move. Nat Rev Mol Cell Biol 2004;5:23–32. [PubMed: 14708007]
21. Carlsson SR, Fukuda M. The lysosomal membrane glycoprotein lamp-1 is transported to lysosomes by two alternative pathways. Arch Biochem Biophys 1992;296:630–639. [PubMed: 1632650]
22. Akasaki K, Michihara A, Fujiwara Y, Mibuka K, Tsuji H. Biosynthetic transport of a major lysosome-associated membrane glycoprotein 2, lamp-2: a significant fraction of newly synthesized lamp-2 is delivered to lysosomes by way of early endosomes. J Biochem (Tokyo) 1996;120:1088–1094. [PubMed: 9010755]
23. Barriocanal JG, Bonifacino JS, Yuan L, Sandoval IV. Biosynthesis, glycosylation, movement through the Golgi system, and transport to lysosomes by an N-linked carbohydrate-independent mechanism of three lysosomal integral membrane proteins. J Biol Chem 1986;261:16755–16763. [PubMed: 3782140]
24. Janvier K, Bonifacino JS. Role of the endocytic machinery in the sorting of lysosome-associated membrane proteins. Mol Biol Cell 2005;16:4231–4242. [PubMed: 15987739]
25. Ho SN, Hunt HD, Horton RM, Pullen JK, Pease LR. Site-directed mutagenesis by overlap extension using the polymerase chain reaction [see comments]. Gene 1989;77:51–59. [PubMed: 2744487]
26. Manders EM, Stap J, Brakenhoff GJ, van Driel R, Aten JA. Dynamics of three-dimensional replication patterns during the S-phase, analysed by double labelling of DNA and confocal microscopy. J Cell Sci 1992;103 (Pt 3):857–862. [PubMed: 1478975]
27. Larocca JN, Almazan G. Acetylcholine agonists stimulate mitogen-activated protein kinase in oligodendrocyte progenitors by muscarinic receptors. J Neurosci Res 1997;50:743–754. [PubMed: 9418962]
28. Le Borgne R, Hoflack B. Protein transport from the secretory to the endocytic pathway in mammalian cells. Biochim Biophys Acta 1998;1404:195–209. [PubMed: 9714803]

29. Hua W, Sheff D, Toomre D, Mellman I. Vectorial insertion of apical and basolateral membrane proteins in polarized epithelial cells revealed by quantitative 3D live cell imaging. J Cell Biol 2006;172:1035–1044. [PubMed: 16567501]
30. Kreitzer G, Schmoranzer J, Low SH, Li X, Gan Y, Weimbs T, Simon SM, Rodriguez-Boulan E. Three-dimensional analysis of post-Golgi carrier exocytosis in epithelial cells. Nat Cell Biol 2003;5:126–136. [PubMed: 12545172]
31. Waguri S, Dewitte F, Le Borgne R, Rouille Y, Uchiyama Y, Dubremetz JF, Hoflack B. Visualization of TGN to endosome trafficking through fluorescently labeled MPR and AP-1 in living cells. Mol Biol Cell 2003;14:142–155. [PubMed: 12529433]
32. Presley JF, Cole NB, Schroer TA, Hirschberg K, Zaal KJ, Lippincott-Schwartz J. ER-to-Golgi transport visualized in living cells [see comments]. Nature 1997;389:81–85. [PubMed: 9288971]
33. Llopis J, McCaffery JM, Miyawaki A, Farquhar MG, Tsien RY. Measurement of cytosolic, mitochondrial, and Golgi pH in single living cells with green fluorescent proteins. Proc Natl Acad Sci U S A 1998;95:6803–6808. [PubMed: 9618493]
34. Kirchhausen T. Adaptors for clathrin-mediated traffic. Annu Rev Cell Dev Biol 1999;15:705–732. [PubMed: 10611976]
35. Davidson HW, Balch WE. Differential inhibition of multiple vesicular transport steps between the endoplasmic reticulum and trans Golgi network. J Biol Chem 1993;268:4216–4226. [PubMed: 8382697]
36. Pind SN, Nuoffer C, McCaffery JM, Plutner H, Davidson HW, Farquhar MG, Balch WE. Rab1 and Ca2+ are required for the fusion of carrier vesicles mediating endoplasmic reticulum to Golgi transport. J Cell Biol 1994;125:239–252. [PubMed: 8163543]
37. Aballay A, Barbieri MA, Colombo MI, Arenas GN, Stahl PD, Mayorga LS. A phorbol ester-binding protein is required downstream of Rab5 in endosome fusion. FEBS Lett 1998;441:373–378. [PubMed: 9891974]
38. Barbieri MA, Li G, Mayorga LS, Stahl PD. Characterization of Rab5:Q79L-stimulated endosome fusion. Arch Biochem Biophys 1996;326:64–72. [PubMed: 8579373]
39. Nuoffer C, Davidson HW, Matteson J, Meinkoth J, Balch WE. A GDP-bound of rab1 inhibits protein export from the endoplasmic reticulum and transport between Golgi compartments. J Cell Biol 1994;125:225–237. [PubMed: 8163542]
40. Puertollano R, Randazzo PA, Presley JF, Hartnell LM, Bonifacino JS. The GGAs promote ARF-dependent recruitment of clathrin to the TGN. Cell 2001;105:93–102. [PubMed: 11301005]
41. Bonifacino JS, Traub LM. Signals for sorting of transmembrane proteins to endosomes and lysosomes. Annu Rev Biochem 2003;72:395–447. [PubMed: 12651740]
42. Futter CE, Connolly CN, Cutler DF, Hopkins CR. Newly synthesized transferrin receptors can be detected in the endosome before they appear on the cell surface. J Biol Chem 1995;270:10999–11003. [PubMed: 7738042]
43. Polishchuk EV, Di Pentima A, Luini A, Polishchuk RS. Mechanism of constitutive export from the golgi: bulk flow via the formation, protrusion, and en bloc cleavage of large trans-golgi network tubular domains. Mol Biol Cell 2003;14:4470–4485. [PubMed: 12937271]
44. Mogelsvang S, Marsh BJ, Ladinsky MS, Howell KE. Predicting function from structure: 3D structure studies of the mammalian Golgi complex. Traffic 2004;5:338–345. [PubMed: 15086783]
45. Le Borgne R, Hoflack B. Mannose 6-phosphate receptors regulate the formation of clathrin-coated vesicles in the TGN. J Cell Biol 1997;137:335–345. [PubMed: 9128246]
46. Puertollano R, Aguilar RC, Gorshkova I, Crouch RJ, Bonifacino JS. Sorting of mannose 6-phosphate receptors mediated by the GGAs. Science 2001;292:1712–1716. [PubMed: 11387475]
47. Larocca J, Ortiz E, Demoliner K, Si Q, Rodriguez. Oligodendrocyte vesicle transport: interaction of rRab22b and OCRL-1. Journal of Neurochemistry 8222005;94(Suppl 2):30.Ref Type: Generic
48. McPherson PS, Garcia EP, Slepnev VI, David C, Zhang X, Grabs D, Sossin WS, Bauerfeind R, Nemoto Y, De Camilli P. A presynaptic inositol-5-phosphatase. Nature 1996;379:353–357. [PubMed: 8552192]
49. Ng EL, Wang Y, Tang BL. Rab22B's role in trans-Golgi network membrane dynamics. Biochem Biophys Res Commun 2007;361:751–757. [PubMed: 17678623]

50. Pfeffer S. A model for Rab GTPase localization. Biochem Soc Trans 2005;33:627–630. [PubMed: 16042559]
51. Zerial M, McBride H. Rab proteins as membrane organizers. Nat Rev Mol Cell Biol 2001;2:107–117. [PubMed: 11252952]
52. Allan BB, Moyer BD, Balch WE. Rab1 recruitment of p115 into a cis-SNARE complex: programming budding COPII vesicles for fusion [see comments]. Science 2000;289:444–448. [PubMed: 10903204]
53. Echard A, Jollivet F, Martinez O, Lacapere JJ, Rousselet A, Janoueix-Lerosey I, Goud B. Interaction of a Golgi-associated kinesin-like protein with Rab6. Science 1998;279:580–585. [PubMed: 9438855]
54. Nakagawa T, Setou M, Seog D, Ogasawara K, Dohmae N, Takio K, Hirokawa N. A novel motor, KIF13A, transports mannose-6-phosphate receptor to plasma membrane through direct interaction with AP-1 complex. Cell 2000;103:569–581. [PubMed: 11106728]
55. Holloway ZG, Grabski R, Szul T, Styers ML, Coventry JA, Monaco AP, Sztul E. Activation of ADP-ribosylation factor regulates biogenesis of the ATP7A-containing trans-Golgi network compartment and its Cu-induced trafficking. Am J Physiol Cell Physiol 2007;293:C1753–C1767. [PubMed: 17913844]
56. Bannykh SI, Plutner H, Matteson J, Balch WE. The role of ARF1 and rab GTPases in polarization of the Golgi stack. Traffic 2005;6:803–819. [PubMed: 16101683]
57. Miaczynska M, Zerial M. Mosaic organization of the endocytic pathway. Exp Cell Res 2002;272:8–14. [PubMed: 11740860]

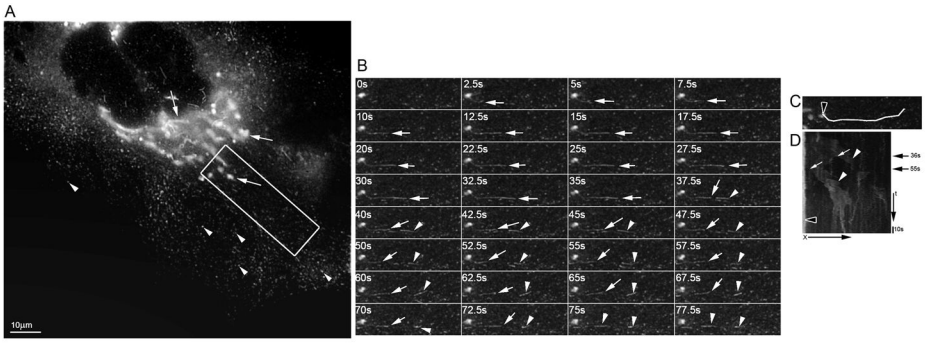

Figure 1. Dynamics of formation in the TGN of carriers containing Rab31

HeLa cells expressing Rab31-ECFP were transferred to recording medium, and the formation and the transport of post-Golgi carriers containing Rab31-ECFP at 32° C was monitored by time-lapse fluorescence microscopy. Images were captured at 0.5 sec intervals. **A)** Fluorescence pattern distribution. Rab31-ECFP localized in the TGN (arrow), and in small structures throughout the cytoplasm (arrowhead). **B)** Individual frames of the area boxed in (A). A TGN tubule extends (white arrow), and its tip breaks up to form a carrier (white arrowhead, 37.5 sec frame). The remaining tubule seems to retract, then again to extend and break up to form a second carrier (white arrowhead, 75 sec frame). Time in sec relative to the first image is shown. **C)** Area where the events in B occurred (carrier formation and movement to cell periphery) is indicated by a white lane. Black arrowhead shows carrier formation site. **D)** Kymograph analysis of the area defined in (C). A lack of movement of the TGN compartments results in a vertical trace (black arrowhead). Diagonal trace represents the formation of carrier and its movement through the area. Two white arrows indicate sequential breaking up of the TGN tubule to form two carriers (white arrowheads). The slope of the trace indicates speed of movement. Black arrows on the right indicate the time of budding in (B). X, distance in µm; t, time in sec.

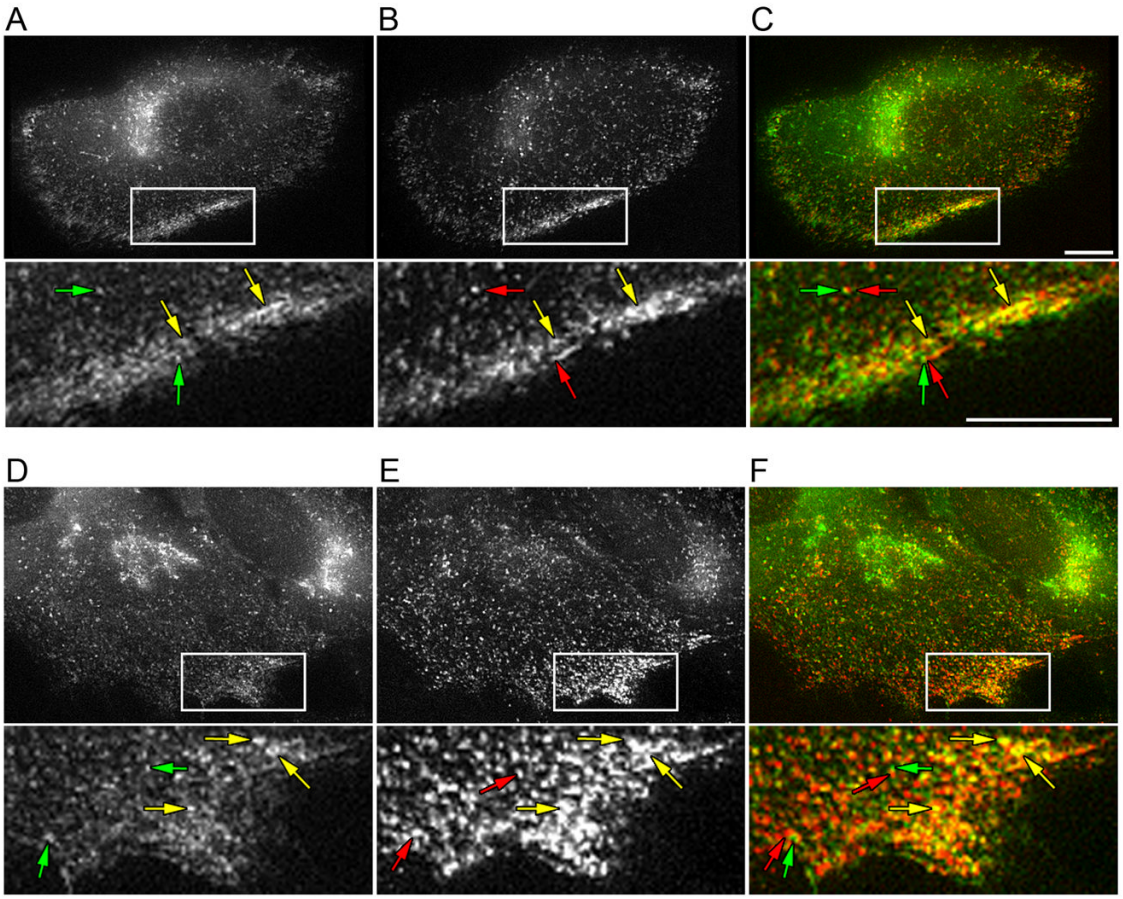

Figure 2. Rab31 is present in endosomes

HeLa cells expressing Rab31-ECFP were incubated for 2 hours at 37° C in medium without FCS, but containing 0.2% BSA. Then cells were incubated with Texas Red transferrin (20 μg/ml) for 15–20 min. After incubation with fluorescent transferrin, cells were rinsed briefly in phosphate buffered saline (PBS) at 4°C and then fixed with 4 % paraformaldehyde in PBS at 4°C for 15 min. Cells were rinsed with PBS and analyzed by double fluorescence microscopy. **A and D,** Rab31-ECFP; **B and E**, Texas Red transferrin; **C** overlap of A and B, and **F** overlap of D and E. Texas Red Transferrin, Red; Rab31-ECFP, green; and overlapping of Texas Red Transferrin and Rab31-ECFP, yellow. Small panels are a 3.33 × magnification of the areas highlighted by white boxes. Compartments containing Rab31-ECFP (green arrows) are tightly associated with compartments containing Texas Red Transferrin (red arrows). Endosomal compartments containing both labels are present in the cell periphery (yellow arrows).

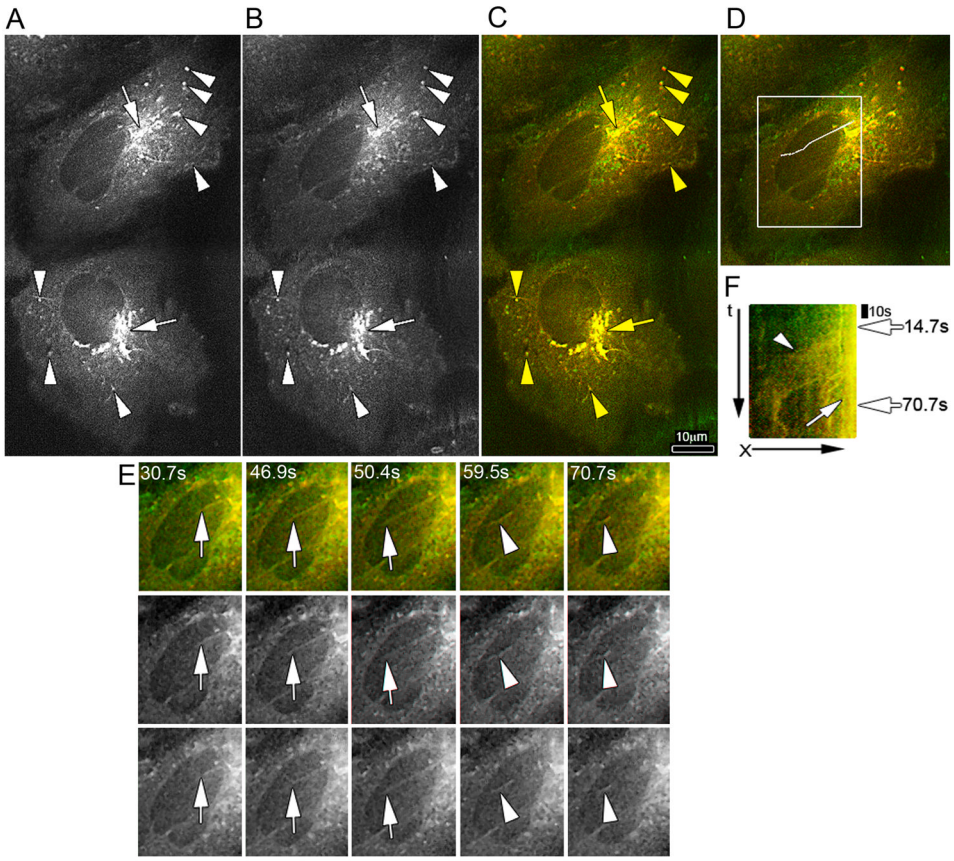

Figure 3. Rab31 is present in carriers that transport CD-MPR from TGN to endosomes

HeLa cells expressing CD-MPR-ECFP were transfected with a plasmid encoding Rab31-EYFP. Forty eight hours after transfection, cells were transferred to recording medium, and the formation and the transport of post-Golgi carriers were monitored at 32° C by time-lapse fluorescence microscopy. Images were collected every 0.70 sec. Fluorescence pattern distribution; **A)** CD-MPR-ECFP, **B)** Rab31-EYFP and **C)** overlapping of A and B, CD-MPR-ECFP (red), Rab31-EYFP (green), and overlapping of CD-MPR-ECFP and Rab31-EYFP (yellow). Rab31-EYFP and CD-MPR-ECFP co-localized in the TGN (arrow), and in small tubolo vesicular compartments throughout the cytoplasm (arrowhead). **D)** Area of the cells shown in E is marked by a white box. Area where the events in E occurred (carrier formation and movement to cell periphery) is indicated by a white lane. **E)** Individual frames showing a TGN tubule that extends (white arrow), and breaks up to form a carrier containing both CD-MPR-ECFP and Rab31-EYFP (white arrowhead). Rab31-EYFP, bottom panels; CD-MPR-ECFP, center panels and merged images top panels (color code, the same as in C). Time in sec relative to the first image is shown. **F)** Kymograph analysis of the area defined in (D). TGN compartments, vertical trace (white arrow). Carrier formation and its movement, diagonal trace (arrowhead). White arrows on the right indicate when the budding showed in (E) occurred. X, distance in μm; t, time in sec.

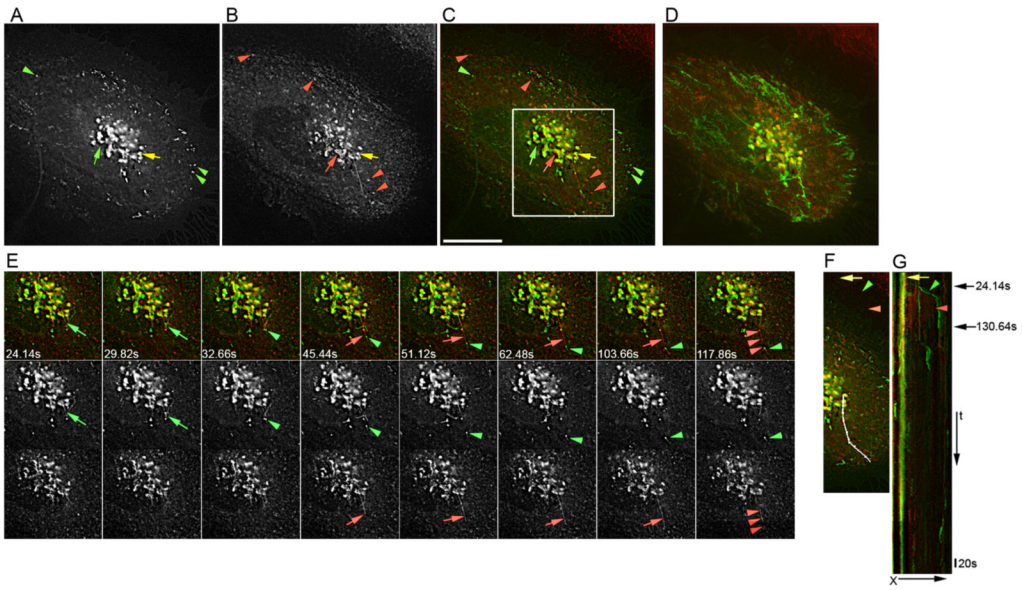

Figure 4. Rab31 and newly synthesized CD63 are sorted in the TGN into different carriers

HeLa cells expressing Rab31-ECFP were micro-injected intranuclearly with cDNAs encoding CD63-EYFP. Newly synthesized CD63-EYFP was trapped in the TGN and carrier formation was visualized by time-lapse double florescence microscopy. Images were collected every 1.42 sec. Fluorescence distribution pattern: A) CD63-EYFP, B) Rab31-ECFP and C) merged images. Green, CD63-EYFP; red, Rab31-ECFP; yellow, overlapping of CD63-EYFP; and Rab31-ECFP. Rab31-EYFP and CD63-ECFP co-localized in some TGN domains (yellow arrow), other TGN domains contain only CD63-EYFP (green arrow) or Rab31-ECFP (red arrow). Small vesicles present in the cytoplasm only contain Rab31-ECFP (red arrow heads) or CD63-EYFP (green arrow heads). **D)** Maximum pixel projection. Rab22b-ECFP and CD63-EYFP co-localized in the TGN but not in small vesicles present throughout the cytoplasm. **E)** Individual frames of the area marked with a box in (C). Top panels, merged images; center panels, CD63-EYFP and bottom panels, Rab31-ECFP. A TGN tubule containing CD63-EYFP extends (green arrow), and breaks up to form a carrier (green arrowhead). Then a long TGN tubule containing Rab31-ECFP extends along the same trajectory (red arrow), and simultaneously breaks in several regions to form three carriers (red arrowheads). **F)** Area where the events in E occurred (carrier formation and their movement to cell periphery) is indicated by a white lane. **G)** Kymograph analysis of the area defined in (F). TGN compartments, vertical traces (yellow arrow). The green trace that corresponds to the budding of carrier containing CD63-EYFP seen in (B) is indicated by a green arrowhead. The wide red trace corresponding to the formation of three carriers containing Rab31-ECFP is indicated by a red arrow. Black arrows on the right indicate the time when the budding occurred. The time in sec relative to the first image is shown. X, distance in μm; t, time in sec. Bar, 10 μm.

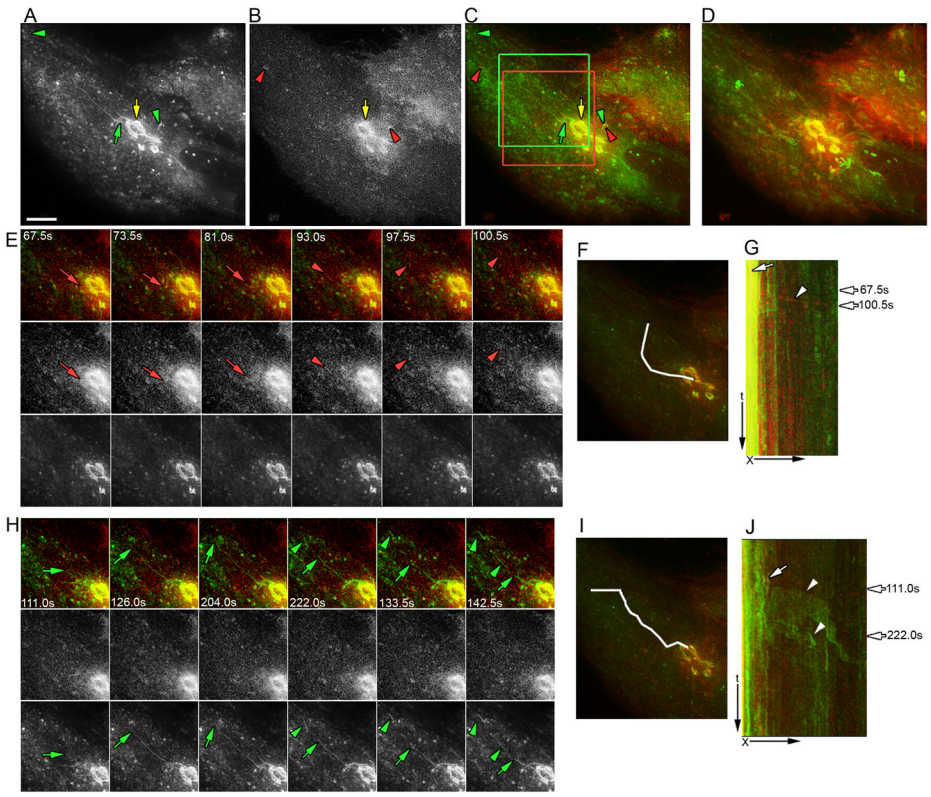

Figure 5. Rab31 and newly synthesized VSVG are sorted into different carriers in the TGN

HeLa cells expressing Rab31-ECFP were transfected with plasmid encoding VSVG-Venus, and then incubated at 40° C for 10–12 hrs. to accumulate VSVG-Venus in the ER. Transfected cells were then incubated at 20° C for 3 hrs, with cycloheximide (100 μg/ml) to trap VSVG-Venus in the TGN. The cells were transferred to recording media at 32 ° C to induce transport of VSVG from Golgi to PM. Time lapse photographs visualized the formation of carriers containing Rab31-ECFP and of carriers containing VSVG-Venus. Images were collected every 1.50 sec. Fluorescence distribution pattern: **A)** Rab31-ECFP, **B)** VSVG-Venus and **C)** merged images. Green, Rab31-ECFP; red, VSVG-Venus; yellow, overlapping of VSVG-Venus and Rab31-ECFP. Rab31-ECFP and VSVG-Venus co-localized in some TGN domains (yellow arrow), other TGN domains contain only Rab31-ECFP (green arrow). Small vesicles present in the cytoplasm only contain Rab31-ECFP (green arrow head) or VSVG-Venus (red arrow head). **D)** Maximum pixel projection. Rab22b-ECFP and VSVG-Venus co- localized in the TGN but not in small vesicles present throughout the cytoplasm. **E)** Individual frames of the area marked with red box in (C). Top panels, merged images; center panels, VSVG-Venus; and bottom panels, Rab31-ECFP. A TGN tubule containing VSVG-Venus extends (red arrow), and breaks up to form a carrier (red arrowhead). **F)** Area where the events in E occurred (carrier formation and movement to the cell periphery) is indicated by a white lane. **G)** Kymograph analysis of the area defined in (F). TGN compartments, vertical traces (white arrow). The red trace that corresponds to the budding of carrier containing VSVG-Venus seen in (E) is indicated by a white arrowhead. Arrows on the right indicate the time of budding in (E). **H)** Individual frames of the area marked with green box in (A). A TGN tubule extends (green arrow), and its tip breaks up to form a carrier (green arrowhead, 142.5 sec frame). The remaining tubule seems to retract, then again to extend and break up to form a second carrier (green arrowhead, 222.0 sec frame). Time in sec relative to the first image is shown. **I)** Area where the events in H occurred (carrier formation and movement to cell periphery) is indicated by a white lane. **J)** Kymograph analysis of the area defined in (G). TGN compartments, vertical trace (white

arrow). Carrier formation and its movement, diagonal trace. Two white arrowheads indicate sequential breaking up of the TGN tubule to form two carriers. Arrows on the right indicate the time of budding in (H). X, distance in μm; t, time in sec. Bar, 10 μm.

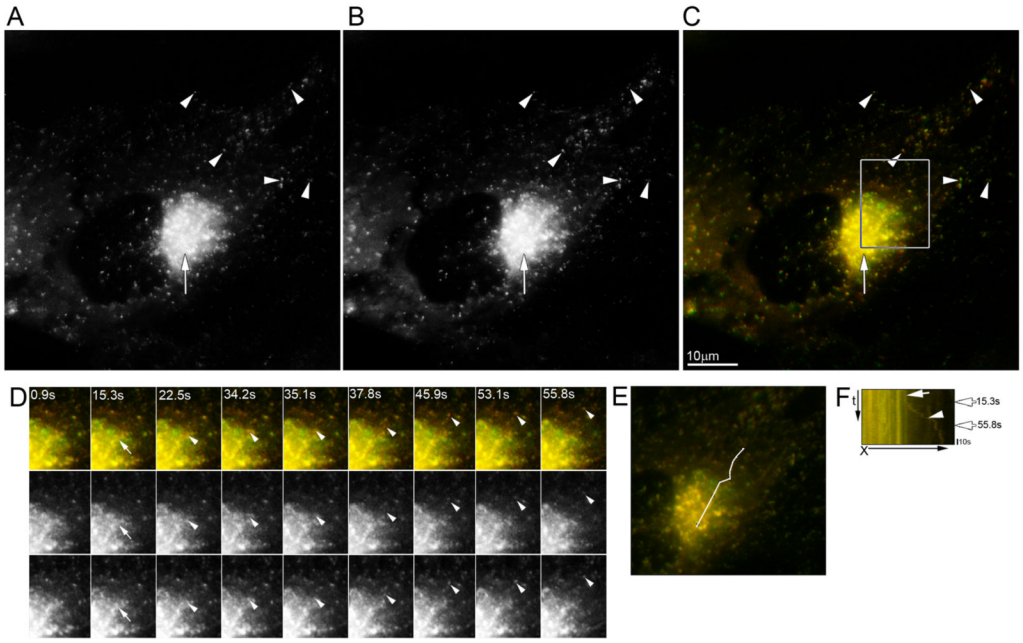

Figure 6. Clathrin coats the carrier vesicles that contain Rab31

HeLa cells expressing clathrin-ECFP were transfected with a plasmid encoding Rab31-EYFP. Cells were transferred to recording medium, and the formation and the movement of post-Golgi carriers was monitored at 30° C by time-lapse fluorescence microscopy. Images were collected every 0.90 sec. Fluorescence pattern distribution; **A)** Rab31-EYFP, **B)** clathrin-ECFP and **C)** merged images. Clathrin-ECFP (red), Rab31-EYFP (green) and overlapping of clathrin-ECFP and Rab31-EYFP (yellow). Rab31-ECFP and clathrin-ECFP co-localize in the TGN (arrow), and in endosomes throughout the cytoplasm (arrowhead). **D)** Individual frames showing formation and movement of a carrier containing both clathrin-ECFP and Rab31-EYFP (white arrowhead). Top panels, merged images; middle panels, Rab31-EYFP; and bottom panels, clathrin-ECFP. Time in sec relative to the first image is shown. **E)** Area where the events in D (carrier formation and movement to cell periphery) occurred is indicated by a white lane. **F)** Kymograph analysis of the area defined in (E). TGN compartments, vertical yellow trace (white arrow). Carrier formation and its movement, diagonal yellow trace (arrowheads). White arrowhead identifies the trace that corresponds to the carrier budding shown in (D). Arrows on the right indicate the time when the budding in (D) occurred. X, distance in μm; t, time in sec. Bar, 10 μm.

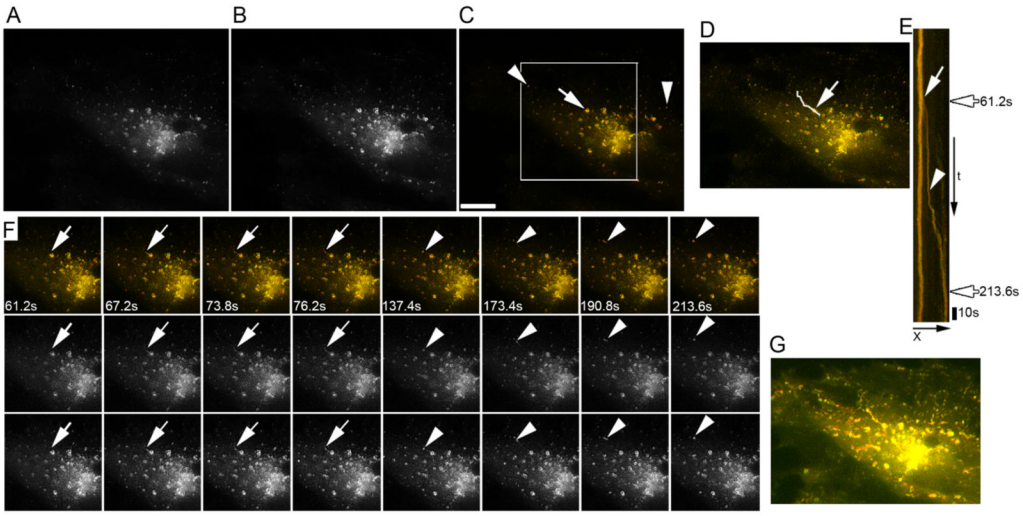

Figure 7. Rab31 and GGA1 colocalize in carriers that bud from the TGN

HeLa cells expressing GGA1-ECFP were transfected with a plasmid encoding Rab31-EYFP. Cells were transferred to recording medium. Formation and the transport of post-Golgi carriers were monitored at 30° C by time-lapse fluorescence microscopy. Images were collected every 0.6 sec. Fluorescence pattern distribution; **A)** Rab31-EYFP, **B)** GGA1-ECFP and **C)** merged images. GGA1-ECFP (red), Rab31-EYFP (green) and overlapping of GGA1-ECFP and Rab31-EYFP (yellow). Rab31-ECFP and GGA1-ECFP co-localize in the TGN (arrow) (r = 0.912 ± 0.012), and in endosomes throughout the cytoplasm (arrowhead) (r = 0.914 ± 0.026). **D**) White lane marks the trajectory of a carrier formed in the TGN. Carrier formation and movement is shown in individual frames (F). **E)** Kymograph analysis of the trajectory mark in (D). TGN compartments, vertical yellow trace (white arrow). Carrier formation and its movement, diagonal yellow trace (arrowheads). White arrowhead identifies the trace that corresponds to carrier budding shown in (F). Arrows on the right indicate the time of budding shown in (F). X, distance in μm; t, time in sec. **F)** Individual frames showing a TGN tubule extending (white arrow), and breaking up to form a carrier containing both GGA1-ECFP and Rab31-EYFP (white arrowhead). Top panels, merged images; center panels, Rab31-EYFP; and bottom panels, GGA1-ECFP. Time in sec relative to the first image is shown. **G)** Maximum pixel projection. Rab22b-EYFP and GGA1-ECFP co- localized in the TGN and in small vesicles present throughout the cytoplasm. Bar, 10 μm.

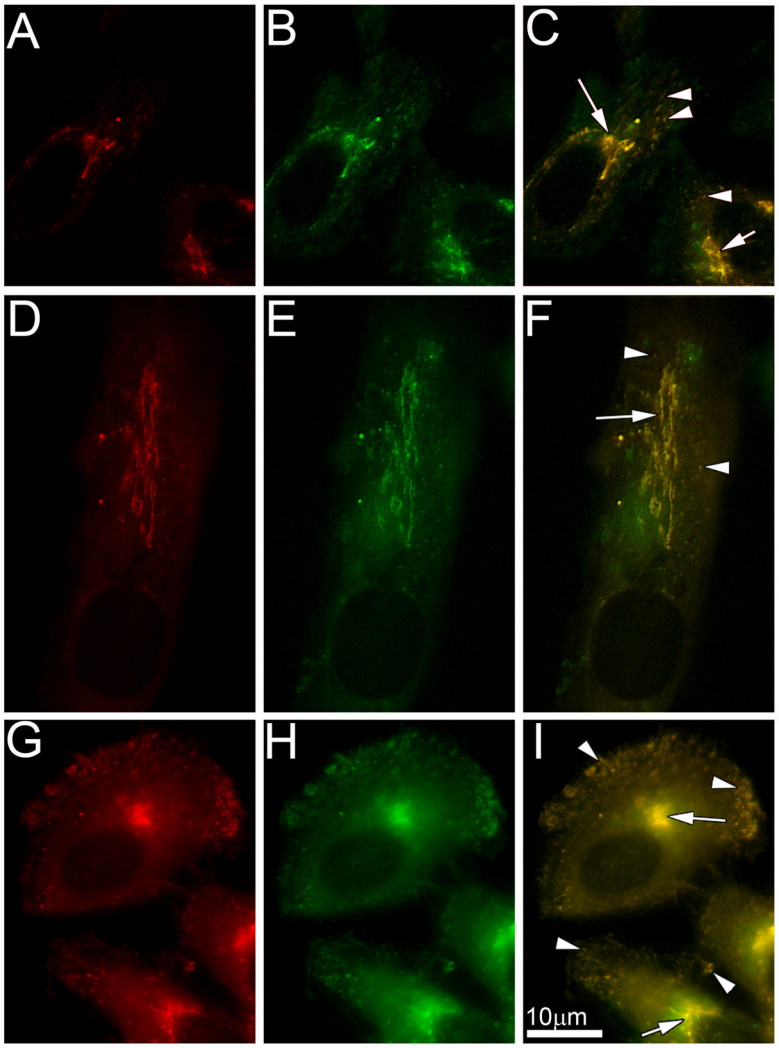

Figure 8. Expression of two Rab31 mutants (S19N and Q64L) result in changes in the quantity of CD-MPR distributed between the TGN and endosomes

(A, B, C) HeLa cells expressing both CD-MPR-ECFP and wild type Rab31-EYFP. **A)** CD-MPR-ECFP (red), **B)** wild type Rab31-EYFP (green) and **C)** overlap of A and B, yellow compartments containing both wild type Rab31-EYFP and CD-MPR-ECFP (TGN, arrow and endosomes, arrowhead). Video 8 C shows that TGN tubules extend and break up to form carriers. **(D, E, F)** HeLa cells expressing both CD-MPR-ECFP and Rab31 (S19N)-EYFP. **D)** CD-MPR-ECFP (red); **E)** Rab31 (S19N)-EYFP (green); **F)** overlap of D and E, yellow compartments containing both Rab31(S19N)-EYFP and CD-MPR-ECFP (Golgi, arrow and endosomes, arrowhead). Notice the large size of the TGN (video 8 F shows that the long TGN tubules do not extent). **(G, H, I)** HeLa cells expressing both CD-MPR-ECFP and Rab31 (Q64L) mutant-EYFP. **G)** CD-MPR-ECFP (red), **H)** Rab31 (Q64L)-EYFP (green) and **I)** overlap of G and H, yellow compartments contain both Rab31(Q64L)-EYFP and CD-MPR-ECFP (Golgi, arrow and endosomes, arrowhead). Notice small size of the TGN and large amount of endosomes in the cell periphery (video 8 I shows that the long TGN tubules extend and break up to form carriers containing both proteins).

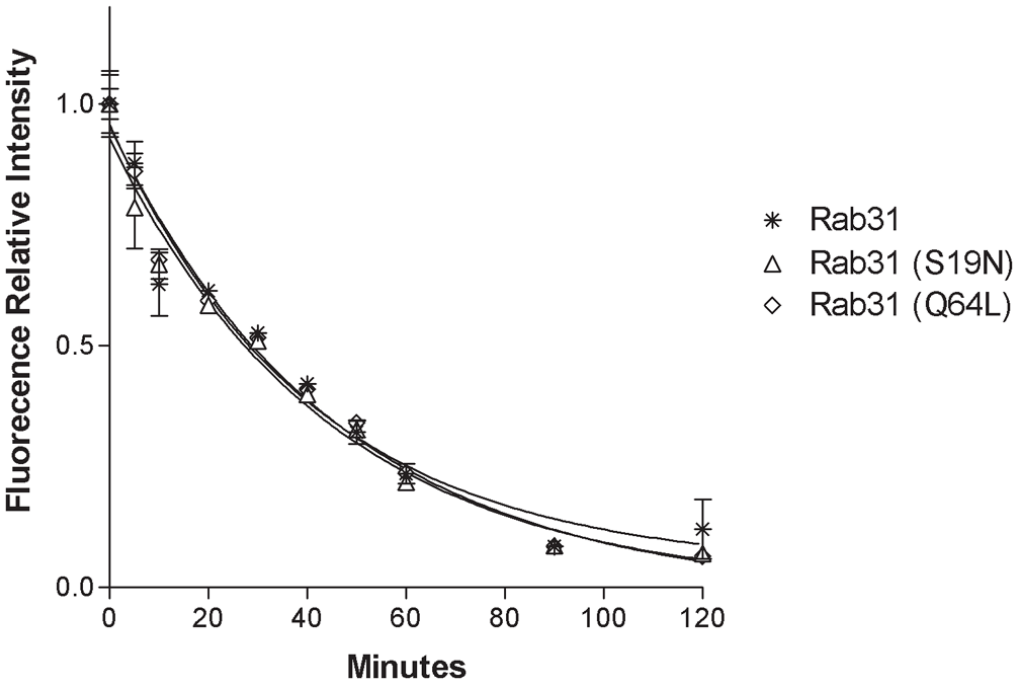

Figure 9. Rate of VSVG-Venus exit from Golgi

HeLa cells expressing either wild type Rab31 or Rab31 (S19N) mutant or Rab31 (Q64L) mutant were transfected with plasmid encoding VSVG-Venus, and maintained for 16 hours at 40° C. Newly synthesized VSVG-Venus was trapped in the Golgi by incubating the cells at 20° C for 3 hours with cycloheximide (100μg/ml). The transport of VSVG from Golgi to PM was induced by shifting the cells to 32° C. The amount of VSVG-Venus fluorescence present in the Golgi at different time periods was determined as described (Materials and Methods). The fluorescence intensities attributable to VSVG-Venus in the Golgi were plotted as a function of time for cells expressing: wild type Rab31 [*], Rab31(S19N) [Δ] and Rab31(Q64L) [◇]. The curves represent the optimized fit to a first order kinetic model. The rate constants obtained by non linear regression analysis were 0.024 ± 0.003 min^{-1}, 0.022 ± 0.003 min^{-1}, 0.021 ± 0.002 min^{-1} respectively; and the half resident times were 28.34 ± 3.27 min, 30.86 ± 3.00 min, 31.65 ± 2.5 min. The values are the means ± standard error for 10 measurements.

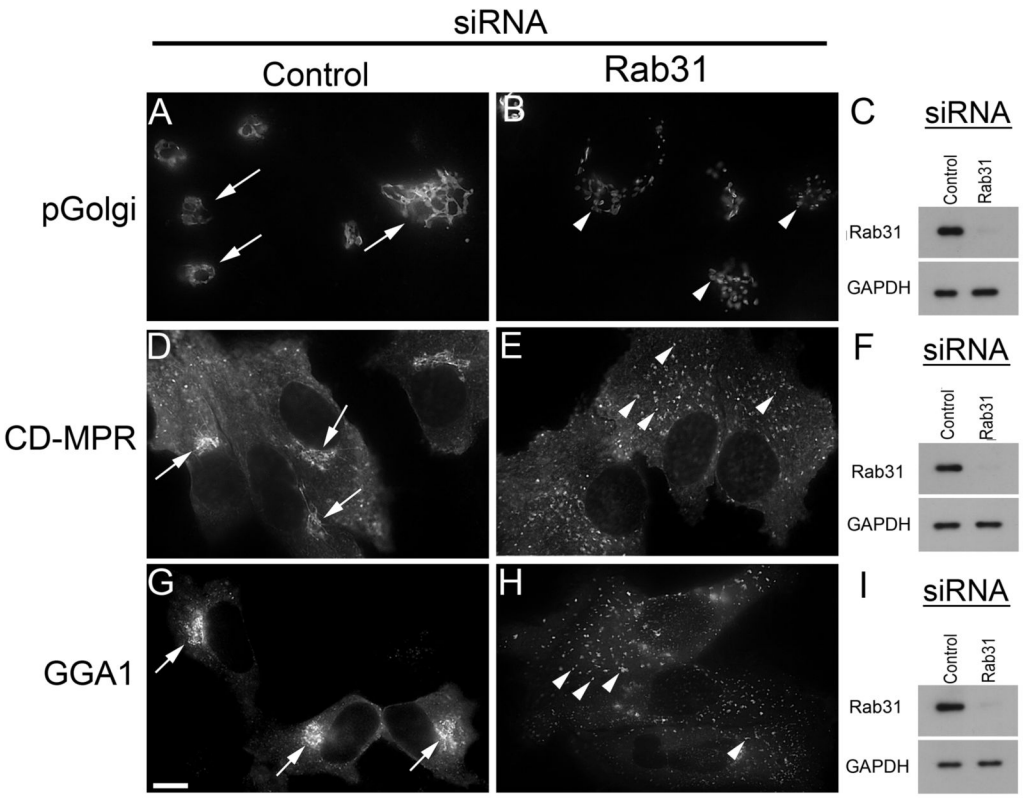

Figure 10. Depletion of endogenous Rab31 fragments Golgi/TGN structure

(A, D and G) HeLa cells were transfected with non targeting siRNA (control), or **(B, E and H)** siRNA that target a segment of the sequence of Rab31 present in exon 2 (5′-GGAUCACUUUGACCACCACAAC-3′). After 48 hrs, the level of Rab31 and GAPDH were determinate from immunoblots **(C, F and I)**. The effect of RNAi depletion on the distribution of pGolgi-ECFP **(A and B)**, CD-MPR-ECFP **(D and E)** or GGA1-ECFP **(G and H)** were analyzed by fluorescence microscopy. **A, D and G**; arrows indicate the position of Golgi/TGN in cells treated with non targeting siRNA. **B, E and H**; arrow heads indicate the position of Golgi/TGN fragments in Rab31 depleted cells. Bar, 10 μm.

Table 1

Effect of Rab31 mutants on the formation of MPR carries from TGN

HeLa cells expressing MPR-ECFP were transfected with plasmid encoding either Rab31-EYFP or Rab31-EYFP (Q64L) mutant or Rab31 (S19N) mutant. Two days later the formation of carriers containing MPR-ECFP was studied by time lapse. Images were captured at 1 sec intervals for a 2 min period. Numerical values are means ± SE. n indicates the number of cells or numbers of carriers. Asterisk marks the value that is statistically significant ($p<0.001$, ANOVA).

Cells expressing	Number of carriers formed in two min	Average speed (μm/sec)
Wild type Rab31	5.55 ± 1.01 (n = 40)	0.81 ± 0.20 (n = 55)
Rab31 (S19N) mutant	0.52 ± 0.09 (n = 52) *	0.78 ± 0.28 (n = 15)
Rab31 (Q64L) mutant	7.00 ± 1.02 (n = 43)	0.85 ± 0.25 (n = 57)